Scientia Iranica, Vol. 12, No. 2, pp 233–240

SCIENTIA
IRANICA

Research Note

Entropy Generation Analysis of a Flat Plate Boundary Layer with Various Solution Methods

J.A. Esfahani* **and M. Malek Jafarian**[1]

Steady state boundary layer equations over a flat plate with a constant wall temperature can be solved by an integral solution (with three profiles for velocity and temperature), a similarity solution (exact) and a Blasius series solution. The analysis of entropy generation for each solution is carried out. The results show that the exact solution (similarity) is the one that minimizes the rate of total entropy generation in the boundary layer. Then, the Blasius solution has the least entropy generation of all. The bell-shaped profile (sinus profile) in the integral solution generates less entropy than the piecewise linear profile, consequently. So, with this method, if the exact solution for a specified problem were not available, one could evaluate the approximate solutions and recognize the best one among them. By introducing a new non-dimensional number (Ej number), which is the ratio of thermal entropy to friction entropy generation, one can recognize which of them is dominant in the boundary layer. Also, it is observed that variation of the total entropy generation is the same as the variation of boundary layer thickness, so, the non-dimensional total entropy generation for various solutions is constant.

INTRODUCTION

Heat transfer phenomena are always accompanied by entropy generation, hence, by the one-way destruction of available work. Therefore, it makes good engineering sense to focus on the irreversibility of heat transfer processes and try to understand the function of the entropy generation mechanism. For example, good heat exchanger design means, ultimately, an efficient thermodynamic performance, which is the least generation of entropy or least destruction of available work (exergy) in the power/refrigeration system incorporating the heat exchanger [1].

The art of adjusting the convection process so that it destroys the least available work (subject to various system constraints) is the focus of the applied field of entropy generation minimization. Fowler and Bejan used a thermo-economic analysis to study the optimal sizes of bodies with specified external forced convection heat transfer [2]. Shuja and Zubair presented a thermo-economic design and optimization of fins with a constant cross-sectional area. This includes capital costs and irreversibility penalty costs [3]. Sahin investigated entropy generation of a laminar flow, flowing in a tube with a constant wall temperature [4]. Also, Esfahani and Baghdar investigated the effect of tube diameter on the optimum length, in the heat transfer process, with constant wall temperature [5]. Walsh et al. developed a quick, simple and, relatively, accurate method for the prediction of entropy in steady, two-dimensional, incompressible, adiabatic boundary layer flows of turbomachines, which gives both the distribution and magnitude of the entropy generation rate [6]. Also, they presented a preliminary optimization analysis, in the laminar region of a non film cooled turbine blade, which demonstrates the concept of how the entropy generation rate may be reduced by varying the boundary layer edge velocity distribution along the suction surface, whilst the work done by the blade is kept constant [7]. Griffin et al. investigated the effect of Reynolds number, compressibility and free stream turbulence on a profile of the entropy generation rate. Increased free stream turbulence had a greater effect on the generated entropy. It was observed that the amount of entropy generated in the turbulent boundary layer was, approximately, equivalent for two turbulence levels at a comparable Reynolds number [8]. Bejan showed that the natural shape of the velocity and temperature profiles of the two-dimensional turbulent jet

*. *Corresponding Author, Department of Mechanical Engineering, Ferdowsi University of Mashad, Mashad, P.O. Box 91755-1111, I.R. Iran.*

1. *Department of Mechanical Engineering, Ferdowsi University of Mashad, Mashad, P.O. Box 91755-1111, I.R. Iran.*

is the one that minimizes the total entropy generation rate [9].

In the present work, the objective is to draw attention to the natural shape of velocity and temperature profiles, which minimize the total entropy generation rate. Hence, boundary layer equations over a flat plate with constant wall temperature were solved by an integral solution (with three profiles for velocity and temperature), a Blasius series solution and a similarity solution (exact solution). Then, the rate of entropy generation for each solution is calculated. The results show that the exact velocity and temperature profile (similarity solution) is the one that minimizes the rate of total entropy generation. The bell-shaped profiles (sinus profile) in the integral solution generates less entropy than the piecewise linear profile, consequently, being closer to the natural shape of the velocity and thermal profiles. So, with this method, if the exact solution for a specified problem were not available, one could evaluate the approximate solutions and recognize the best one among them.

GOVERNING EQUATIONS

Consider the flow over a horizontal flat plate (Figure 1). The governing equations of this physical problem are the steady state boundary layer equations:

$$\frac{\partial u}{\partial x}+\frac{\partial v}{\partial y}=0, \tag{1}$$

$$u\frac{\partial u}{\partial x}+v\frac{\partial u}{\partial y}=\nu\frac{\partial^2 u}{\partial y^2}, \tag{2}$$

$$u\frac{\partial T}{\partial x}+v\frac{\partial T}{\partial y}=\alpha\frac{\partial^2 T}{\partial y^2}, \tag{3}$$

where the velocity changes from $u=0$ to $u=U_\infty$ and the temperature changes from $T=T_w$ to $T=T_\infty$ in a space situated relatively close to the solid wall [10]. There are various methods for solving boundary layer equations. Here, integral, Blasius and similarity solution methods are investigated. In the next section, these methods are briefly reviewed.

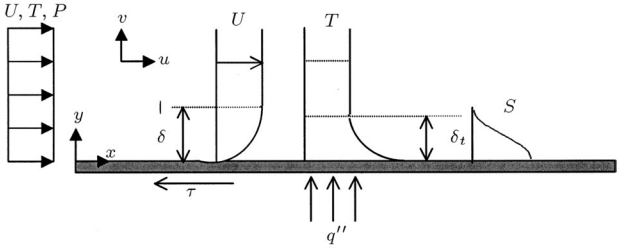

Figure 1. Velocity, temperature and entropy generation boundary layer along a flat plate parallel to a uniform stream.

SOLUTION METHODS

Similarity Solution

In this method, by introducing the similarity solution parameter, the streamline function and the dimensionless similarity temperature profile as [10]:

$$\eta=y\sqrt{\frac{U_\infty}{\nu x}}, \tag{4}$$

$$\psi=\sqrt{U_\infty \nu x}F(\eta), \tag{5}$$

$$\frac{T_w-T}{T_w-T_\infty}=G(\eta), \tag{6}$$

the similarity form of the boundary layer momentum and energy equations are obtained as:

$$F'''+\frac{1}{2}FF''=0, \tag{7}$$

$$\frac{1}{\Pr}G''+\frac{1}{2}FG'=0, \tag{8}$$

with the following boundary conditions:

$$\begin{cases} G=F=F'=0 & \text{at} \quad \eta=0 \\ G,F'\to 1 & \text{as} \quad \eta\to\infty. \end{cases} \tag{9}$$

Blasius Series Solution

The solution of Equation 7 is obtained by Blasius, which satisfies the boundary conditions by the method of matched asymptotic expansions [11]. Esfahani et al. make use of a modal series with the aid of the following dimensionless parameter [12]:

$$\frac{u}{U_\infty}=f'(\eta), \qquad \frac{T_w-T}{T_w-T_\infty}=g(\eta), \tag{10}$$

where the closed form of $f(\eta)$ is defined as:

$$f(\eta)=\sum_{n=0}^{\infty}B_n\alpha^{n+1}\eta^{3n+2}, \tag{11}$$

η is as the same as Equation 4 and:

$$B_n=\frac{-1}{2(3n)(3n+1)(3n+2)}\sum_{k=0}^{n-1}(3k+1)(3k+2)B_kB_{n-k-1}. \tag{12}$$

By replacing $f(\eta)$ into Equation 8 and integration, $g(\eta)$ and $g'(\eta)$ are obtained as:

$$g'(\eta)=\text{Exp}\left(-\frac{1}{2}\text{pr}\sum_{n=0}^{\infty}\frac{B_n\alpha^{n+1}}{3n+3}\eta^{3n+3}-1.22\right),$$

$$g(\eta)=\int_0^{\infty}g'(\eta)d\eta. \tag{13}$$

Integral Solution

Integrating the conservative form of the boundary layer equations from $y = 0$ to $y = Y = \max(\delta, \delta_T)$ and substituting boundary conditions, yields the integral boundary layer equations [10]. Assuming that the shape of the longitudinal velocity and temperature profiles are described by:

$$\begin{cases} \frac{u}{U_\infty} = f(\xi) & 1 \le \xi \le 1 \\ \frac{u}{U_\infty} = 1 & 1 \le \xi \end{cases}, \tag{14}$$

$$\begin{cases} \frac{T_w - T}{T_w - T_\infty} = f(\zeta) & 0 \le \zeta \le 1 \\ \frac{T_w - T}{T_w - T_\infty} = 1 & 1 \le \zeta \end{cases}, \tag{15}$$

f is an unspecified profile shape function that varies from 0 to 1 and $\xi = \frac{y}{\delta}, \zeta = \frac{y}{\delta_T}$, where δ and δ_T are the velocity and thermal boundary layer thicknesses. Substituting these definitions into an integral boundary layer equation for momentum yields:

$$\frac{\delta}{x} = a_1 \mathrm{Re}_x^{-1/2}. \tag{16}$$

The numerical coefficient, a_1, depends on the particular guess made for the profile shape function, f [10]. Assuming that:

$$\frac{\delta_T}{\delta} = \Delta, \tag{17}$$

where Δ is a function of the Prandtl number only and δ is given by Equation 16. Based on these definitions and $\delta_T \le \delta$ ($\mathrm{Pr} > 1$) and substitution into the integral form of the energy equation, one can determine δ_T [10]. Assuming the simplest temperature profile, $f(\zeta) = \zeta$, one has:

$$\Delta = \mathrm{Pr}^{-1/3}. \tag{18}$$

Other choices of profile shape, $f(\zeta)$, will change the proportionality factor in Equation 18 only percentage points. The results for other profile shapes, $f(\xi)$ and $f(\zeta)$, are hinted at by Table 1.

Table 1 shows that the boundary layer thickness is varied with various profile shapes. It is observed that there is a wide difference between the results. The proper velocity and temperature profiles could be the ones that minimize the total entropy generation rate of a flat plate boundary layer. Thus, by calculation of the total entropy generation for various solutions, the more accurate solution and natural shape of profiles can be recognized. In the next section, the methods of entropy generation calculation for various solutions are discussed.

ENTROPY GENERATION

It is easy to show that the rate of a one-way destruction of useful work in an engineering system, W_{lost}, is directly proportional to the rate of entropy generation:

$$W_{\mathrm{lost}} = T_i S_{\mathrm{gen}}, \tag{19}$$

where T_i is the absolute temperature of the ambient reservoir (T_i= constant) [1]. Assuming a finite-size control volume at an arbitrary point in a two-dimensional convection flow field and applying the second law of thermodynamics, the mix entropy generation per unit time and per unit volume (S'''_{gen}) is [10]:

$$S'''_{\mathrm{gen}} = \frac{k}{T^2}\left[\left(\frac{\partial T}{\partial x}\right)^2 + \left(\frac{\partial T}{\partial y}\right)^2\right] + \frac{\mu}{T}\left\{2\left[\left(\frac{\partial u}{\partial x}\right)^2 + \left(\frac{\partial \nu}{\partial y}\right)^2\right] + \left(\frac{\partial u}{\partial y} + \frac{\partial \nu}{\partial x}\right)^2\right\}, \tag{20}$$

where k and μ are the conductivity and viscosity of the fluid. T represents the absolute temperature of the point where S'''_{gen} is being evaluated. Equation 20 illustrates the cooperation between viscous dissipation and imperfect thermal contact in the generation of entropy via convective heat transfer. The entropy generation (Equation 20) can be simplified by scale

Table 1. The impact of profile shape on various solutions of the laminar boundary layer including friction and heat transfer.

Profile Shapes $f(\xi)$ or $f(\zeta)$	$a_1 = \frac{\delta}{x}\mathrm{Re}_x^{1/2}$	$a_2 = \frac{\delta_T}{x}\mathrm{Re}_x^{1/2}\mathrm{Pr}^{1/3}$	$\Delta \mathrm{Pr}^{1/3}$
$f = \xi$	3.46	3.46	1.000
$f = \frac{\xi}{2}(3 - \xi^2)$	4.64	4.53	0.976
$f = \sin\left(\frac{\pi}{2}\xi\right)$	4.80	4.65	0.968
Blasius Solution (18 Terms)	4.90	6.10	1.244
Similarity Solution	5.00	5.60	1.120

analysis for flow over a flat plate with length L:

$$\frac{\partial T}{\partial x} \approx \frac{\Delta T}{L}, \quad \frac{\partial T}{\partial y} \approx \frac{\Delta T}{\delta_T} \quad \rightarrow \quad \frac{\partial T}{\partial x} \langle\langle \frac{\partial T}{\partial y},$$

$$\frac{\partial \nu}{\partial x} \approx \frac{U_\infty \delta}{L^2}, \quad \frac{\partial u}{\partial y} \approx \frac{U_\infty}{\delta} \quad \rightarrow \quad \frac{\partial \nu}{\partial x} \langle\langle \frac{\partial u}{\partial y},$$

$$\frac{\partial u}{\partial x} \approx \frac{U_\infty}{L}, \quad \frac{\partial u}{\partial y} \approx \frac{U_\infty}{\delta} \quad \rightarrow \quad \frac{\partial u}{\partial x} \langle\langle \frac{\partial u}{\partial y}, \tag{21}$$

where $\Delta T = T_w - T_\infty$ is the scale of temperature variation in the region $\delta_T \times L$. Thus, entropy generation can be simplified as:

$$S'''_{\text{gen}} = \frac{k}{T^2}\left(\frac{\partial T}{\partial y}\right)^2 + \frac{\mu}{T}\left(\frac{\partial u}{\partial y}\right)^2. \tag{22}$$

As seen, entropy generation depends on the determining of flow field velocity and temperature. The first term on the right hand side of Equation 22 is called thermal entropy generation and the second term is called friction entropy generation. On the other hand, velocity and temperature profiles depend on the method of solution, which is reviewed in the previous section. In the next section, various methods of solution are evaluated by entropy generation and the accuracy of them is discussed.

Calculation of Entropy Generation with Similarity Solution

Non-dimensional mix entropy generation ($\overline{S}'''_{\text{gen}}$) is introduced as follows:

$$\overline{S}'''_{\text{gen}} = \frac{S'''_{\text{gen}}}{(k/x^2)\text{Re}_x} = \frac{S'''_{\text{gen}}}{k(a_1/\delta)^2}, \tag{23}$$

which is normalized of entropy generation by boundary layer thickness. Using the definition of ψ in Equation 5 to express the derivative of velocity and temperature as:

$$\frac{\partial u}{\partial y} = U_\infty \sqrt{\frac{U_\infty}{\nu x}} F'', \qquad \frac{\partial T}{\partial y} = -\Delta T \sqrt{\frac{U_\infty}{\nu x}} G,' \tag{24}$$

then, by replacing them into Equation 22 and using Equation 23, non-dimensional mix entropy generation can be written in the following form:

$$\overline{S}'''_{\text{gen}} = \left(\frac{\Delta T}{T}\right)^2 G'^2 + \left(\frac{\Delta T}{T}\right).Ec.\text{Pr}.F''^2, \tag{25}$$

where Ec is the Eckert number of the fluid and is defined as below:

$$Ec = \frac{U_\infty^2}{C_p.\Delta T}, \tag{26}$$

T refers to local temperature as:

$$T = T_w - \Delta T.G(\eta). \tag{27}$$

Now, one can define a non-dimensional parameter as below:

$$Ej = \left(\frac{T}{\Delta T}\right).Ec.\text{Pr}, \tag{28}$$

where it is the ratio of non-dimensional friction entropy generation per thermal entropy generation. To create the Ej number, Equation 25 is rearranged as:

$$\overline{S}'''_{\text{gen}} \left(\frac{\Delta T}{T}\right)^{-2} = G'^2 + Ej.F''^2.$$

A large Ej number shows that friction entropy generation is more than the thermal entropy generation in the boundary layer and vice versa for a small Ej number.

Calculation of Entropy Generation with Blasius Solution

By derivation from velocity and temperature profiles defined in Equation 10, one has:

$$\overline{S}'''_{\text{gen}} = \left(\frac{\Delta T}{T}\right)^2 \text{Exp}\left(-\text{Pr}\sum_{n=0}^{\infty}\frac{B_n \alpha^{n+1}}{3n+3}\eta^{3n+3} - 2.44\right)$$

$$+\left(\frac{\Delta T}{T}\right).Ec.\text{Pr}.\left(\sum_{n=0}^{\infty}(3n+1)(3n+2)B_n\alpha^{n+1}\eta^{3n}\right)^2, \tag{29}$$

where:

$$T = T_w - \Delta T.g(\eta). \tag{30}$$

Calculation of Entropy Generation with Integral Solution

Using the definition of the velocity and temperature profiles in Equations 14 and 15, one has:

$$\overline{S}'''_{\text{gen}} = \left(\frac{\Delta T}{T}\right)^2 \left(\frac{\text{Pr}^{1/3}}{a_2}\frac{\partial f}{\partial \zeta}\right)^2$$

$$+\left(\frac{\Delta T}{T}\right).Ec.\text{Pr}.\left(\frac{1}{a_1}\frac{\partial f}{\partial \xi}\right)^2, \tag{31}$$

where:

$$T = T_w - \Delta T.f(\zeta), \tag{32}$$

δ and δ_T are obtained from Table 1 for various profile shapes.

It should be mentioned that all the results discussed here are for air over a flat plate with the following characteristics, unless the characteristics expressed are in the text:

$$\nu = 15.89 \times 10^{-6} \ \frac{\mathrm{m}^2}{\mathrm{s}}, \quad \mu = 184.6 \times 10^{-7} \ \frac{\mathrm{N.s}}{\mathrm{m}^2},$$

$$k = 26.3 \times 10^{-3} \ \frac{\mathrm{w}}{\mathrm{m.k}}, \quad \mathrm{Pr} = 0.707, \quad T_w = 320 \ \mathrm{K},$$

$$T_\infty = 300 \ \mathrm{K}, \quad U_\infty = 10 \ \frac{\mathrm{m}}{\mathrm{s}},$$

where T_w, T_∞ and U_∞ are the wall temperature, the free stream temperature and the free stream velocity, respectively. Based on data mentioned above, the value of the Ej number is 0.054, where it explains that thermal entropy generation is higher than friction entropy generation in the boundary layer at these conditions.

RESULTS AND DISCUSSION

Figure 2 shows the distribution of friction, thermal and mixed entropy generation functions in the boundary layer ($x = 0.5$). The results are obtained by the Blasius series solution. The value of the friction term is very small (about one, near the wall), in contrast to the thermal term (about eleven, near the wall) and confirms the low Ej number described earlier. Also, it is seen that the ratio of friction to thermal entropy generation is about 0.1, which confirms the magnitude of the Ej number. Low values of the Ej number correspond to the low viscosity or low velocity of the fluid. It is clear that by choosing a high viscosity or a high velocity, the contribution of the friction term will be significant. This is shown in Figure 3, where the velocity of the fluid is 100 m/s and other conditions are the same as earlier. At this condition,

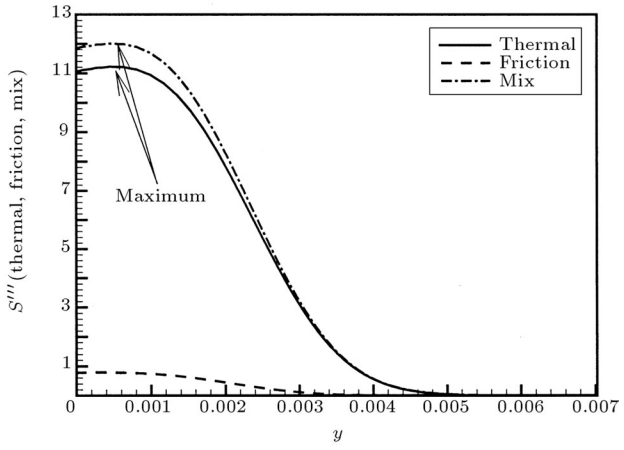

Figure 2. Distribution of entropy generation for Blasius solution ($T_w = 320, T_\infty = 300, U_\infty = 10$, heating).

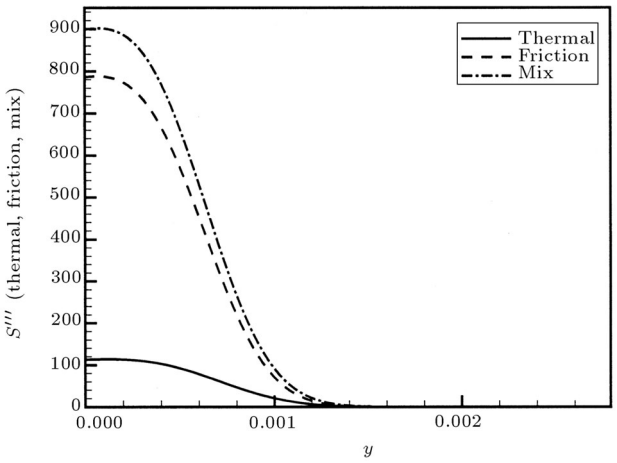

Figure 3. Distribution of entropy generation for Blasius solution ($T_w = 320, T_\infty = 300, U_\infty = 100$, heating).

the Ej number is 5.44, which can be supported by the ratio of $\frac{800}{100}$ in Figure 3. Thus, friction entropy generation is greater than thermal entropy generation. It is seen that the Ej number is a suitable parameter for evaluating the significance of entropy generation components in the boundary layer. Also, three curves in Figures 2 and 3 have a maximum value at a point near the wall (not on the wall). This is observed for the other solutions too. Whenever the wall is cooled by the fluid, the maximum and minimum values of the fluid temperature are on the wall and the edge of the boundary layer, respectively. On the other hand, the slope of the temperature curve reduces from the wall to the edge of the boundary layer. Therefore, heat diffusion decreases, so that the maximum value of the heat diffusion will be on the wall ($y = 0$). Now, with attention to the definition of the entropy generation ($dS'''_{\mathrm{gen}} = \frac{\delta Q}{T}$), marching in a y direction will have a reduction in δQ and T. Therefore, the denominator is trying to increase and the numerator is trying to decrease entropy generation, so that, near the wall, the difference between the denominator and the numerator will have the least value. That will be the maximum entropy generation point.

Figure 4 shows the total entropy generation function, which is determined, as follows, for various solutions:

$$S'''_{\mathrm{gen}}\Big|_{\mathrm{total}} = \sum_{y=0}^{\max(\delta,\delta_T)} \sum_{x=0}^{L} S'''_{\mathrm{gen}}. \tag{33}$$

It is seen that the total entropy generation of the similarity solution is smaller than the other solutions and is the most for a linear profile (rough estimation) in the integral solution. Third order and sinus profiles in the integral solution method are very close, so their profiles have overlapped. The non-dimensional total

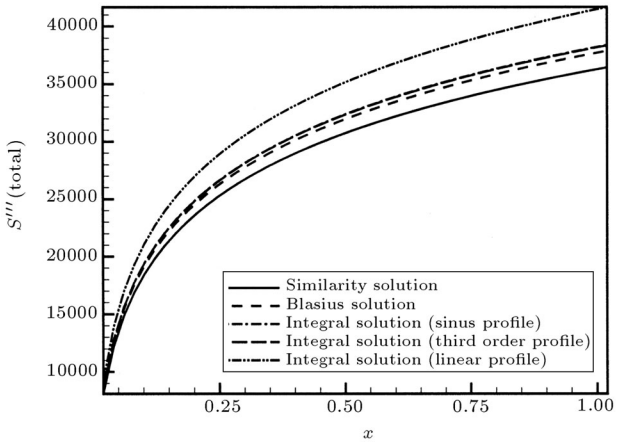

Figure 4. Total entropy generation for various solutions ($T_w = 320, T_\infty = 300, U_\infty = 10$, heating).

entropy generation function is defined as:

$$\overline{S}'''_{\text{gen}}\Big|_{\text{total}} = \sum_{y=0}^{\max(\delta,\delta_T)} \sum_{x=0}^{L} \overline{S}'''_{\text{gen}}, \tag{34}$$

and its distribution is shown in Figure 5. It is seen that the distribution of this parameter is constant for various solutions. This means that variation of total entropy generation is the same as variation of the boundary layer thickness. As observed in Figure 4, the non-dimensional total entropy of the similarity (exact) solution has the least value, then, the Blasius and integral solutions, respectively. The most value is for the linear profile in the integral solution.

Distribution of thermal entropy generation for various solutions is compared in Figure 6 ($x = 0.5$). Entropy generation of the linear profile has minimum value on the wall in comparison to the other solutions. The reason is related to the slope of the temperature curves. The slope of the linear profile is less than the slope of the other profiles (Table 1).

On the other hand, the value of $\frac{k}{T^2}$ is constant for

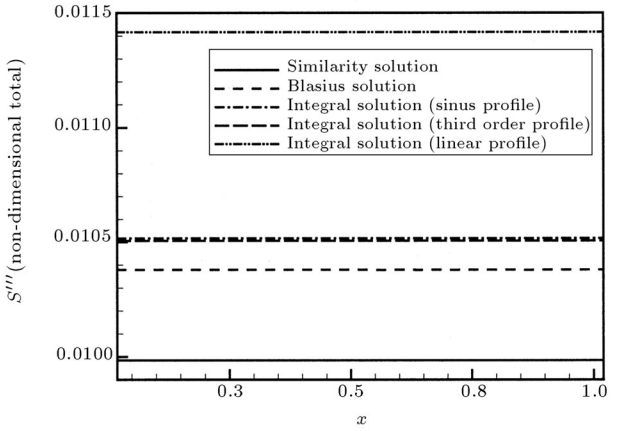

Figure 5. Non-dimensional total entropy generation for various solutions ($T_w = 320, T_\infty = 300, U_\infty = 10$, heating).

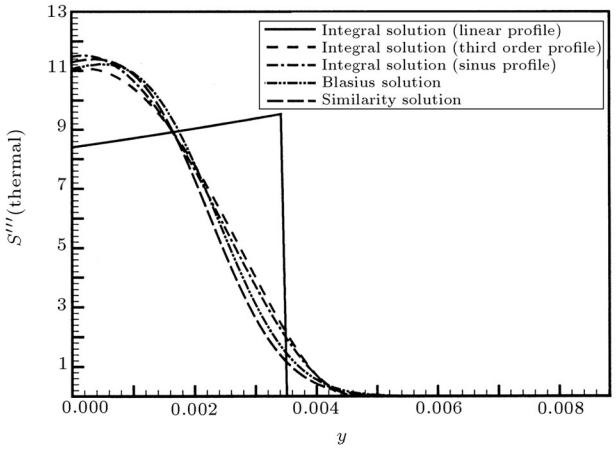

Figure 6. Distribution of thermal entropy generation for various solutions ($T_w = 320, T_\infty = 300, U_\infty = 10$, heating).

various solutions on the wall. Therefore, the thermal entropy generation of a linear profile will be less than the other solutions on the wall. But, moving from the wall ($y > 0.0018$), this trend will be reversed. At the edge of the boundary layer ($y > 0.0042$), a similar trend that is observed near the wall will appear. As seen from Table 1, the thermal boundary layer thickness for a linear profile is less than the other profiles of integral, similarity and Blasius solutions. Therefore, the temperature gradient, as well as the thermal entropy generation, will reach zero at a shorter distance from the wall. Globally, thermal entropy generation has the least value for a similarity solution in the boundary layer thickness. Then, the Blasius solution, the integral solution with sinus and third order and linear profiles have the smallest entropy generation, respectively.

Distribution of thermal entropy generation for various solutions is shown in Figure 7 ($x = 0.5$), where the wall temperature is less than the fluid temperature (cooling conditions). It is seen that the maximum entropy generation occurs on the wall

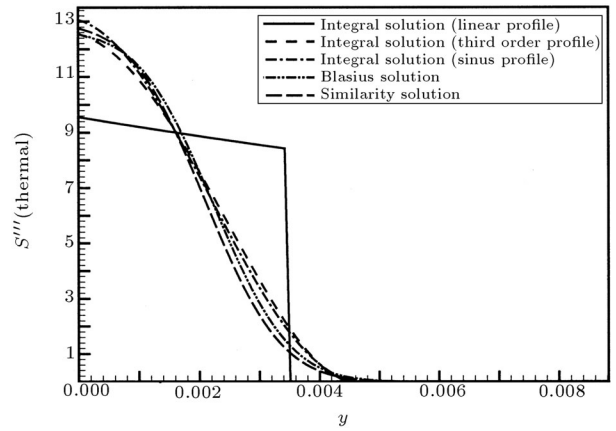

Figure 7. Distribution of thermal entropy generation for various solutions ($T_w = 300, T_\infty = 320, U_\infty = 10$, cooling).

($y = 0$). Marching in a y direction (toward the wall), will have a reduction in T and an increase in δQ. Therefore, the denominator and the numerator are trying to increase entropy generation, so that, on the wall, maximum entropy generation is obtained. But, in view of quantum, there is a similar trend to that of the heating case, shown in Figure 6.

Figure 8 shows the friction entropy distribution in the boundary layer at the heating condition, which is similar to the thermal entropy generation shown in Figure 6. The same trend is observed near the wall and at the edge of the boundary layer, i.e., the minimum value on the wall and the entropy generation of the linear profile tends to zero faster than the other solutions. This is because of the small slope and small boundary layer thickness of the linear profile, in comparison with other profiles, which reminds one that $\frac{\mu}{T}$ is constant on the wall in Equation 22.

Friction entropy generation at the cooling phenomena for various solutions is shown in Figure 9. The same trend observed in the thermal entropy generation of the cooling condition, is seen here. Globally, at the cooling phenomena, the similarity solution has the least value and, then, the Blasius solution.

The authors believe that because the similarity solution is the exact solution, its entropy generation is the least. Therefore, any profile, which produces entropy generation closer to the result of the similarity solution, is the most accurate estimation of all. Here, it is observed that the Blasius solution, with 18 terms, is a better estimation than the integral solutions.

CONCLUDING REMARKS

The entropy generation analysis of a flat plate boundary layer with a constant wall temperature was carried out using three solution methods. Based on this work, the following conclusions can be drawn:

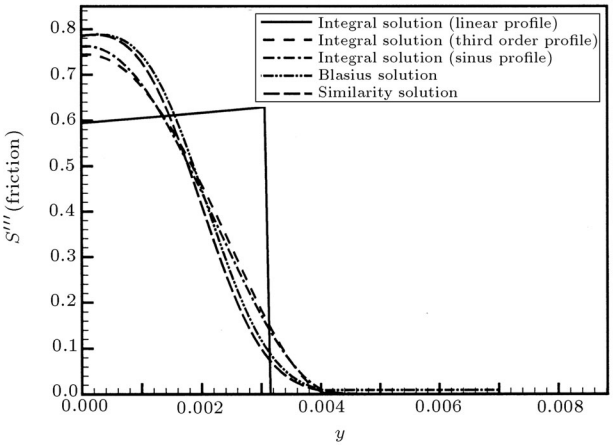

Figure 8. Distribution of friction entropy generation for various solutions ($T_w = 320, T_\infty = 300, U_\infty = 10$, heating).

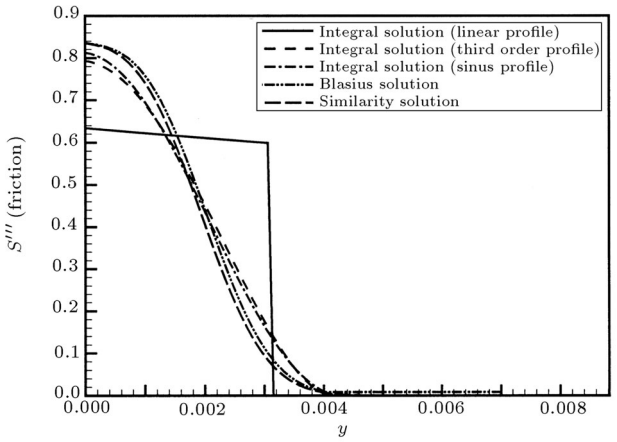

Figure 9. Distribution of friction entropy generation for various solutions ($T_w = 300, T_\infty = 320, U_\infty = 10$, cooling).

- The exact solution (similarity) produced less total entropy generation than the other solutions. Then, the total entropy generation of the Blasius solution and the sinus profile in the integral method was the least, respectively;
- If there is not an exact solution for a problem, one can recognize the best solution, among approximate solutions, with an entropy generation analysis;
- The variation of total entropy generation is the same as the variation of boundary layer thickness;
- The non-dimensional total entropy generation of all solutions is constant;
- By introducing a non-dimensional number (Ej number), one can recognize that one of the thermal entropy and friction entropy generation is dominated in the boundary layer;
- For the heating phenomena (when the wall temperature is higher than the fluid temperature), the maximum entropy generation (thermal and friction) occurs near the wall (not on the wall). But, for the cooling phenomena, this maximum lies on the wall.

From this work, one can recommend the analysis of entropy generation as procedure for evaluating solution methods in the field of thermo-fluid problems.

REFERENCES

1. Bejan, A., *Entropy Generation Through Heat and Fluid Flow*, chapter, 2, New York, USA (1982).
2. Fowler, A.J. and Bejan, A. "Correlation of optimal sizes of bodies with external forced convection heat transfer", *International Communication in Heat and Mass Transfer*, **21**, pp 17-27 (Jan.-Feb. 1994).
3. Shuja, S.Z. and Zubair, S.M. "Thermoeconomic optimization of constant cross-sectional area fines", *ASME Journal of Heat Transfer*, **119**(4), p 860 (1997).

4. Sahin, A.S. "Second law analysis of laminar viscous flow through a duct subjected to constant wall temperature", *ASME Journal of Heat Transfer*, **120**, pp 76-83 (1998).
5. Abolfazli Esfahani, J.A. and Baghdar, F. "Entropy generation analysis of convective heat transfer through fully developed, laminar, viscous flow with a duct subjected to constant wall temperature", *Journal of School of Engineering*, Ferdowsi University of Mashhad, **2**, pp 85-98 (2001).
6. Walsh, E., Myose, R. and Davies, M. "A prediction method for the local entropy generation rate in a transitional boundary layer with a free stream pressure gradient", *Stokes Research Institute*, American Society of Mechanical Engineers, International Gas Turbine Institute, Turbo Expo (Publication) IGTI, **3A**, pp 637-646 (2002).
7. Walsh, E., Davies, M. and Myose, R. "An entropic minimization technique for turbine blade profiles", American Society of Mechanical Engineers, International Gas Turbine Institute, Turbo Expo (Publication) IGTI, **5A**, pp 199-206 (2002).
8. Griffin, P.C., O'Donnell, F.K., Davies, M. and Walsh, E. "The effect of Reynolds number, compressibility and free stream turbulence on profile entropy generation rate", American Society of Mechanical Engineers, International Gas Turbine Institute, Turbo Expo (Publication) IGTI, **5A**, pp 61-69 (2002).
9. Bejan, A. "Thermodynamic of an isothermal flow: The two-dimensional turbulent jet", *Int. J. Heat Mass Transfer*, **34**, pp 407-413 (1991).
10. Bejan, A., *Convection Heat Transfer*, 2nd Ed., John Wiley & Sons, chapter 2 (1993).
11. Schlichting, G.H. "Boundary layer theory", Translated by Kestin, J., 4th Ed., McGrow Hill, pp 116-122 (1960).
12. Esfahani, J.A., Pariz, N. and Abdollahi, A. "Series solution of boundary layer along a plate by modal series approximation", *Proceeding of the 4th Iranian Aerospace Society Conference*, Amir Kabir University of Technology, pp 366-374 (Jan. 2003).